

**SYNTHESIS, CHARACTERIZATION
AND UTILIZATION OF
FORMALDEHYDE-BASED RESINS
MANUFACTURED USING SOME
LOCALLY AVAILABLE PLANT
BASED TANNIN SOURCES**

SELLADURAI ARASARETNAM

Ph.D

2010

**Synthesis, Characterization and
Utilization of formaldehyde-based resins
manufactured using some locally
available plant based tannin sources**

Selladurai Arasaretnam

**Thesis submitted to the University of Sri
Jayewardenepura for the award of the
Degree of Doctor of Philosophy in Chemistry in
2010**

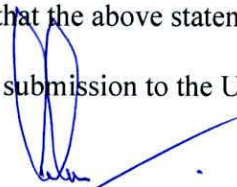
DECLARATION

I do hereby declare that the work described in this thesis was carried out by me under the supervision of Dr. Laleen Karunanayaka and Dr. Susil J. Silva and a report on this has not been submitted in whole or part to any university or any other institution for another Degree/Diploma.

Date: 20/10/2010


Signature of Candidate

We certify that the above statement made by the candidate is true and that this thesis is suitable for submission to the University for the purpose of evaluation.



Dr. Laleen Karunanayake
Senior Lecturer in Chemistry
Department of Chemistry
University of Sri Jayewardenepura
Nugegoda
Sri Lanka
Date: 20/10/2010



Dr. Susil J. Silva
Senior Lecturer in Chemistry
Department of Chemistry
University of Sri Jayewardenepura
Nugegoda
Sri Lanka
Date: 20/10/2010.

We certify that the candidate is submitting this thesis with all corrections, additions and amendments have been done in accordance with the comments and suggestions of the examiners.



Dr. Laleen Karunanayake
Department of Chemistry



Dr. Susil J. Silva
Department of Chemistry



DEDICATION

“Dedicated to my loving Mother and Wife”

LIST OF PUBLICATIONS ARISING FROM THIS THESIS

1. S Arasaretnam and L Karunanayake. Synthesis, Characterization and metal adsorption properties of tannin-phenol-formaldehyde resins produced using tannin from dried fruit of *Terminalia chebula* (Aralu), *Journal of Applied Polymer Science*, USA, 115, 1081-1088, 2010.
2. S Arasaretnam and L Karunanayake. Synthesis, characterisation and metal adsorption of Tannin Phenol Formaldehyde resin obtained from flower buds of *Terminalia chebula*. *Sri Lanka Association for the Advancement of Science*, Proceedings of the 64th, Annual Sessions, part 1, 169, 2008.
3. S Arasaretnam, L Karunanayake, P Manoharan. Formaldehyde based resins prepared using tannin obtained from bark of *Terminalia arjuna* (Roxb.). *Sri Lanka Association for the Advancement of Science*, Proceedings of the 62nd Annual Sessions, part 1, 127-128, 2006.

LIST OF ABBREVIATIONS

TF	Tannin-Formaldehyde
TPF	Tannin-Phenol-Formaldehyde
PTR	Pine type Tannin-formaldehyde Resin
PF	Phenol-Formaldehyde
DFT	Density Functional Theory
UV-Vis	Ultraviolet-Visible
TLC	Thin Layer Chromatography
DSC	Differential Scanning Calorimetry
FTIR	Fourier Transform Infra Red spectra
NMR	Nuclear Magnetic Resonance
HPLC	High Performance Liquid Chromatography
DVB	Divinylbenzene
CSA	Chemical Shift Anisotropy
MAS	Magic Angle Spinning
CP	Cross-Polarization
SBO	Soya Bean Oil
ESBO	Epoxidised Soya Bean Oil
HF	Hartree-Fock
B3LYP	Becke-style 3-Parameter Density Functional Theory (using the Lee-Yang-Parr correlation functional)
FC	Folin-Ciocalteu
TPF_SO ₃ H	Sulfonated-Tannin-Phenol-Formaldehyde
IEC	Ion Exchange Capacity
K _d	Distribution coefficient

SEM	Scanning Electron Microscopic
η	Viscosity
M_n	Number average molecular mass
M_c	Critical molar mass
T_g	Glass transition temperature
KF	Freundlich isotherm constant
KL	Adsorption energy constant of Langmuir adsorption isotherm
q_e	Equilibrium solid phase adsorbate concentration (mg/g)
E_a	Arrhenius activation energy (J/mol)
ΔG°	Gibbs free energy (kJ/mol)
ΔH°	Enthalpy (kJ/mol)
ΔS°	Entropy (J/mol K)
t	Time (h)
T	Absolute temperature ($^\circ\text{C}$)
F/P	Formaldehyde/Phenol ratio
AAS	Atomic Absorption Spectroscopy
Meq	Milli equivalent
C_e	Equilibrium liquid phase concentration (mg/l)
C_o	Initial liquid phase concentration (mg/l)
TDDFT	Time-dependent DFT

TABLE OF CONTENTS

LIST OF TABLES	VIII
LIST OF FIGURES	X
ACKNOWLEDGEMENT	XV
ABSTRACT	XVI
CHAPTER 1: INTRODUCTION	
1.1. Introduction to tannin	1
1.2. Adsorption and Ion Exchange	6
1.3. Rheology study	9
1.4. Epoxidation of oils	11
1.5. Anionic exchanger	11
1.6. Computational Chemistry approach	13
1.6.1. Computational study to predicting the reactivity of polyphenolic compounds with formaldehyde	13
1.6.2. UV Spectroscopic calculations on flavan-3-ol type molecules	13
1.7. Scientific scope of the project (overall and specific objectives)	15
1.7.1 Overall objectives	15
1.7.2 Specific objectives	15
CHAPTER 2: LITERATURE REVIEW	
2.1. Tannins	17
2.1.1. Overview	17
2.1.2 Condensed and Hydrolysable Tannins	18

2.1.3. Tannin Sources	20
2.1.4. Metal chelating properties of Tannins	21
2.2. Tannin-Formaldehyde (TF) and Tannin-Phenol-Formaldehyde (TPF) resin	22
2.3. Phenol-Formaldehyde (PF)	24
2.4. Characterization of Thermoset	25
2.4.1. Overview of Thermoset Cure	25
2.4.2. Conventional DSC	25
2.4.3. Solid-state NMR Spectroscopy	26
2.4.3.1. Overview	26
2.4.3.2. Solid-state NMR Signal-Enhancing Techniques	28
2.4.3.2.1. High-Power Dipolar Decoupling (DD)	28
2.4.3.2.2. Magic Angle Spinning (MAS)	28
2.4.3.2.3. Cross-polarization (CP)	29
2.4.4. Ultraviolet-Visible spectroscopy	29
2.4.5. High Performance Liquid Chromatography (HPLC)	30
2.4.6. Infra-Red Spectroscopy	32
2.5. Ion Exchangers	34
2.5.1. Definition and Principles	34
2.5.2. Theory and mechanism	34
2.5.2.1. Crystal Lattice Theory	34
2.5.2.2. Double Layer Theory	35
2.5.2.3. Donnan Membrane Theory	35
2.6. Modified polystyrene matrices	37
2.7. Strongly Acidic Cation-Exchange Resins	38

2.8. Ion-Exchange Reactions; Cation Exchange	38
2.9. Treatment of Potable Water	38
2.10. Pharmaceutical applications	39
2.11. Ion exchange adsorption isotherms	40
2.12. Epoxidation of vegetable oil	41
2.13. Anionic exchanger using TPF resin	42
2.14. Applications of Computational Chemistry	43
2.14.1. An overview of Computational Chemistry	43
2.14.2. Electronic Structure Methods	44
2.14.3. Density Function Methods	45
CHAPTER 3: METHODS AND METHODOLOGY	
3.1. Materials and Chemicals	47
3.2. Development of a protocol for extraction of tannin	47
3.2.1. Extraction of tannin	47
3.2.2. Separation of Tannin	48
3.3. Characterisation of tannins	49
3.3.1. Determination of pH and viscosity	49
3.3.2. Thin Layer Chromatography (TLC)	49
3.3.3. Determination of tannin content using Folin-Ciocalteu reagent (FC) method	50
3.3.4. HPLC technique	51
3.4. Synthesis for formaldehyde based resins	52
3.4.1. Preparation of Tannin-Phenol-Formaldehyde (TPF) resin	52

3.4.2. Preparation of Sulfonated-Tannin-Phenol-Formaldehyde (TPF_SO ₃ H) resins	53
3.4.3. Preparation of metal adsorbed-Tannin-Formaldehyde resins	54
3.4.4. Preparation of Gallic acid-Formaldehyde (GF) resins	54
3.4.5. Preparation of Phenol-Formaldehyde (PF) resin	55
3.5. Characterization of synthesized resins	56
3.5.1. Free Formaldehyde Determination	56
3.5.2. Determination of Gel Time (t_{gel}) of Tannin/Formaldehyde mixtures using a Rheology study	56
3.5.3. Swelling Property	57
3.5.4. Study of Hydration	57
3.6. Study for Ion Exchange Capacity (IEC) of the synthesised resins	58
3.6.1. Determination of Ion Exchange Capacity of the resins for bivalent cations	58
3.6.2. Contribution of SO ₃ H and OH groups of the Cation Exchanger	59
3.6.3. Effect of pH on ion exchange capacity of resins	59
3.6.4. Effect of electrolyte concentration and pH on distribution coefficients of metal ions	60
3.6.5. Effect of metal ion concentration on Exchange Capacity	61
3.6.6. Determination of Ion Exchange Capacity of the resins for mono valent cations	62
3.7. Differential Scanning Calorimetry (DSC)	62
3.8. Assignment of ¹³ C Solid-state NMR signals	63

3.9. Study on adsorption isotherms	63
3.9.1. Adsorption kinetics and effect of initial pH	63
3.9.2. Effect of temperature on Zn ²⁺ adsorption	64
3.10. Scanning Electron Microscopic (SEM) study for synthesized resins	64
3.11. Studies on applications of synthesised TPF resins	64
3.11.1. Softening of Hard water	64
3.11.2. Amino acid intake properties of the synthesised resin	64
3.12. Epoxidation of Soyabean vegetable oil (SBO)	65
3.12.1. Determination of Epoxy Oxygen Content	66
3.12.2. Characterisation of SBO oil/its derivative	67
3.13. Synthesis of Anionic resin	67
3.13.1. Optimization of reaction conditions for quaternization	67
3.13.2. Determination of Ion Exchange Capacity of the converted resins using phosphate ion	68
3.14. Methods for Computational Chemistry Approach	68
3.14.1. Reactivity of gallic acid and pine type tannin molecules towards HCHO	68
3.14.2. UV Spectroscopic calculations on flavan-3-ol type molecules	71

CHAPTER 4: RESULTS AND DISCUSSION

4.1. Development of Tannin Extraction Method	74
4.2. Analysis of extracted tannin	80
4.2.1. TLC analysis	81
4.2.2. FTIR analysis of dried fruit and its' extracts for Aralu	83
4.3. UV-Visible spectrophotometry analysis	84

4.4. HPLC analysis	86
4.5. Phenol-Formaldehyde resins (PF)	86
4.6. Tannin-Phenol-Formaldehyde (TPF) resins	88
4.7. Determination of the gel time using Rheology study	91
4.8. Ion exchange features	94
4.8.1. ¹³ C Solid-state NMR analysis	105
4.8.2. Effect of pH on metal ion uptake	110
4.8.3. Effect of metal ion concentration on exchange capacity	111
4.8.4. Effect of electrolyte concentration and pH on distribution coefficients of metal ions	112
4.8.5. Swelling properties	114
4.8.6. Hydration properties	114
4.8.7. Stability of the resin sulfonates	116
4.8.8. Ion exchange capacities with respect to mono valent ions	116
4.9. Ion Exchange Capacity Isotherm	119
4.9.1. Adsorption kinetics and effect of initial pH	119
4.9.2. Sorption isotherms	124
4.9.3. Isotherm of Zn ²⁺ on temperature	126
4.10. Adsorption Studies; Surface analysis. Observation of the resin using a Scanning Electron Microscope (SEM)	128
4.11. Studies on Applications of prepared Tannin-Phenol-Formaldehyde Based Cation Exchange Resins	129
4.11.1. Softening of Hard Water	129
4.11.2. The Determination of Amino acids with Ninhydrin	130

4.12. Characterisation of Soyabean oil (SBO)/ Epoxidised Soyabean oil (ESBO)	133
4.12.1. Effect of temperature on epoxidation	134
4.12.2. Kinetics of epoxidation	138
4.13. Anionic resin study	142
4.14. Computational Chemistry	146
4.14.1. Reactivity of gallic acid and pine type tannin molecules	146
4.14.2. UV Spectroscopic calculations on flavan-3-ol type molecules	152
CHAPTER 5: CONCLUSIONS	155
CHAPTER 6: FUTURE RESEARCHES	157
REFERENCES	158
APPENDIXES	

LIST OF TABLES

Table 2.1. Different levels of theory	46
Table 3.1. Label of synthesized resin matrix and weight ratio of Tannin to Phenol	53
Table 3.2. Reaction conditions of phenol-formaldehyde resin synthesis	55
Table 4.1. Amount of the tannin extracted from different nature of Aralu sample	82
Table 4.2. HPLC results for isolated Aralu tannin	86
Table 4.3. Properties of TPF resins	89
Table 4.4. Coefficients a and b at different temperatures	92
Table 4.5. Solubility behaviour of extracted tannin/ synthesised resins in different solvents	97
Table 4.6. Data of materials used and resins obtained	98
Table 4.7. Ion Exchange Capacities of unsulfonated and sulfonated resins for five bivalent cations and molar ratio of $-\text{SO}_3\text{H}$ group to adsorbed metal ion (M^{2+})	103
Table 4.8. K_d values of metal ions in NaCl solution at various molarities and pH	113
Table 4.9. Swelling Vs. Mesh Size	114
Table 4.10. Study of Hydration	115
Table 4.11. Study of Deterioration of Exchange Capacity with Time	116
Table 4.12. Ion Exchange Capacities with Respect to M^+ ions	117
Table 4.13. Exchange Capacities in meq/g for H^+/Na^+ and $\text{H}^+/\text{Pb}^{2+}$ exchange Cycles	118
Table 4.14. Fitted values of the parameters k and $X_{A\text{max}}$ of equation (11)	122
Table 4.15. Variation of adsorption with various initial concentration of Zn^{2+} solution at different temperatures	127

Table 4.16. Freundlich parameters of Zn^{2+} adsorbed on resin at different temperatures	128
Table 4.17. Hardness of Water Before and After Treatment with the synthesised Resin	129
Table 4.18. Chemical properties of epoxidation products of SBO at different temperatures	137
Table 4.19. Levels of epoxidation and rate constant of epoxidation of SBO at various temperatures	139
Table 4.20. Adsorption of phosphate ions at 20 mmol dm^{-3} concentrations by modified ART1P0.5SO ₃ H resin and a commercial anion exchange resins (Amberlite IRA-400)	145
Table 4.21. Mulliken charges distribution obtained by PM3 method in gallic acid	146
Table 4.22. Calculated Mulliken charges at RHF/PM3 level for the pine type tannin formaldehyde molecules with varying number of CH ₂ OCH ₂ cross links	150
Table 4.23. Distribution of charges in a pine type flavanoid unit with Zn^{2+} ion as a ligand	152
Table 4.24. Wavelengths and oscillator strengths for singlet states of compounds (A)-(D)	153
Table 4.25. Wavelength for maximum absorption of band I for compounds (A)-(D)-singlet	154

LIST OF FIGURES

Figure 1.1. Structure of gallic acid and the numbering of its' atoms	1
Figure 1.2. Structure of a flavanoid unit: A-ring: R ₁ =H for resorcinol and R ₁ =OH for phloroglucinol; B-ring: R ₂ =H for pyrocatechol and R ₂ =OH for pyrogallol	2
Figure 1.3. Reaction of galloyl group with formaldehyde. (a) methylation reaction of galloyl unit; (b-d) condensation reaction path of galloyl unit in gallic acid	3
Figure 1.4. $2\text{H}^+ \longleftrightarrow \text{M}^{2+}$ ion exchange between a flavanoid unit and a divalent metal (M^{2+}) ion.	4
Figure 1.5. Reaction of pine type flavanoid unit with formaldehyde	4
Figure 1.6. (A). Four basic flow types of liquids. (1). Newtonian (2). Shear-thickening (3). Shear-thinning (4). Bingham plastic (B) . Schematic diagram of typical shear-thinning behavior (2)	10
Figure 2.1. Structures of the flavonoids	18
Figure 2.2. Structures of common condensed tannin monomers found in fruits and bark	19
Figure 2.3. Structure of simple condensed tannin	19
Figure 2.4. Structure of hydrolysable tannin; gallic acid and glucose	20
Figure 2.5. Structure of a condensed tannin monomer, catechin, binding to a ferrous ion at the <i>o</i> -diphenolic group in the B-ring	21
Figure 2.6. Schematic molecular structure of tannin-phenol-formaldehyde resin	23
Figure 2.7. (a). Proton-carbon dipolar coupling in an isolated C-H bond. (b). Magic angle spinning (MAS) geometry	27
Figure 2.8. Continuous wave Fourier transforms spectrograph	32
Figure 2.9. Structure of a cation exchanger that exchanges H^+ for Na^+ ions, Swelling water is represented in the inset	36

Figure 2.10. Modified cationic polystyrene resin	37
Figure 2.11. Structure of epoxidised soyabean oil	41
Figure 3.1. Gallic acid formaldehyde molecule with single CH ₂ link	70
Figure 3.2. Gallic acid formaldehyde molecule with single CH ₂ OCH ₂ link	70
Figure 3.3. Tannin-formaldehyde molecule with single CH ₂ OCH ₂ link	70
Figure 3.4. A Zinc ion complexed with a flavanoid unit	71
Figure 3.5. B3LYP/6-31+ G* minimum energy conformations	72
Figure 4.1. Percentage of tannins extracted Vs solvent (methanol) to solute (water) ratio at 80 °C	75
Figure 4.2. Effect of temperature (°C) on the extractability of tannins	76
Figure 4.3. Effect of pH on the extractability of tannins in aqueous methanol at 80 °C	77
Figure 4.4. Extraction efficiency of five solvents on Tannin extraction (Values are the average of two replications)	79
Figure 4.5. Extracted tannin compounds on TLC plate	80
Figure 4.6. Extracted tannin from 80 % methanol (ATMe80) on TLC plates under 254nm lamp (a) and 354 nm lamp (b)	81
Figure 4.7. TLC on 80 % methanol extract from different nature of Aralu sample	82
Figure 4.8. TLC on 80 % methanol extract from Aralu dried fruit and standards of Gallic acid & Catechin	83
Figure 4.9. FTIR spectra of dried fruit and dried fruit extracts for Aralu sample	84
Figure 4.10. UV spectrum for gallic acid(1), isolated tannins(2) and catechin(3)	85
Figure 4.11. IR spectra of phenol and PF resin	87
Figure 4.12. Relative IR absorption of the reference peak Vs Time at 80 °C	88
Figure 4.13. ln η_0 Vs ln t	92

Figure 4.14. Variation of $1/\eta_0$ as a function of time of the system tannin extract + 37 % formaldehyde solution during curing at 65 °C	94
Figure 4.15. Extent of sulfonation (related to Ion Exchange Capacity) vs. Time	95
Figure 4.16. FTIR spectra of tannin-formaldehyde, phenol-modified and its sulfonated resin	99
Figure 4.17. FTIR spectra of the ART1P0.5SO ₃ H resin and its metal complexed form	101
Figure 4.18. Glass transition temperatures (T_g) of virgin, sulfonated and Pb-adsorbed resins obtained from the DSC thermograms	104
Figure 4.19(a). ¹³ C solid-state NMR spectrum of the extracted tannin sample	106
Figure 4.19(b). ¹³ C solid-state NMR spectrum of the tannin-phenol- formaldehyde resin	107
Figure 4.19(c). ¹³ C solid-state NMR spectrum of the sulfonated tannin-phenol-formaldehyde resin	108
Figure 4.19(d) ¹³ C solid-state NMR spectrum of the metal adsorbed (Mg ²⁺) sulfonated tannin-phenol-formaldehyde	109
Figure 4.20. Effect of pH on metal ion exchange capacity	111
Figure 4.21. Effect of concentration on metal ion exchange capacity	112
Figure 4.22. pH neutralization curve of ART1P0.5SO ₃ H	118
Figure 4.23. Effect of contact time on the sorption of cation on ART1P0.5SO ₃ H resin and on the pH of the solution: (a) 100 mg/l Mg ²⁺ , pH ₀ = 8.2 ; (b) 750 mg/l Pb ²⁺ , pH ₀ = 5.5 [(■) X _A ; (◆)pH]	120
Figure 4.24. Kinetics of the sorption of Mg ²⁺ and Pb ²⁺ on ART1P0.5SO ₃ H resin at 30 °C from solutions with various initial pH (a) 100 mg/l Mg ²⁺ , (▲) pH ₀ = 8.2; (■) pH ₀ = 7.2 ; (◆) pH ₀ = 6.8 (b) 750 mg/l Pb ²⁺ , pH ₀ = 5.5 (◇);pH ₀ = 5.1(□);pH=4.5(△)	123
Figure 4.25. Effect of initial pH on the sorption of Mg ²⁺ (Top) and Pb ²⁺ (Bottom)	124

Figure 4.26. Freundlich Isotherm for adsorption of Pb^{2+} on to resin at 30 °C	125
Figure 4.27. Langmuir Isotherm for adsorption of Pb^{2+} on to resin at 30 °C	125
Figure 4.28. Freundlich isotherms for Zn^{2+} on ARTPSO ₃ H resin at different temperatures	127
Figure 4.29. Calibration curve of Phenyl aniline	131
Figure 4.30. Calibration curve of Glutamic acid	132
Figure 4.31. FTIR Spectra of SBO and ESBO	133
Figure 4.32. FTIR spectra: spectra of SBO and ESBO prepared at various temperature reacting for 6 hours (H: ESBO at 45 °C, I: ESBO at 50 °C, J: ESBO at 60 °C, K: ESBO at 70 °C)	135
Figure 4.33. Extent of epoxidation of SBO by ART1P0.5SO ₃ H resin at various temperatures	136
Figure 4.34. FTIR spectra: spectra of oleic acid and epoxidized oleic acid prepared at various temperature reacting for 6 hours	137
Figure 4.35. Kinetics of epoxidation of SBO by synthesized ART1P0.5SO ₃ H resin	139
Figure 4.36. Activation energy, E_a for the epoxidation of SBO by ART1P0.5SO ₃ H resin	140
Figure 4.37. $\ln(K/T)$ Vs $1/T$	141
Figure 4.38. Phosphate (P) adsorption by quaternized ART1P0.5SO ₃ H resin prepared in the presence of different NaOH concentrations	142
Figure 4.39. Phosphate (P) adsorption by quaternized ART1P0.5SO ₃ H resin prepared in the presence of different ratios of NaOH to trimethylammonium chloride	143
Figure 4.40. Phosphate (P) adsorption by quaternized ART1P0.5SO ₃ H resin prepared at different reaction times	144

Figure 4.41. Variation of Mulliken charges of the reactive carbon at the tail of the gallic acid molecules linked with CH_2 and CH_2OCH_2 in the gallic acid formaldehyde polymer	147
Figure 4.42. FTIR spectra of gallic acid polymer before curing (Ga_HCHO_prepolymer) and gallic acid polymer after curing at 100°C (Ga_HCHO polymer)	148
Figure 4.43. FTIR spectra of pine type tannin (PT) and pine type tannin-formaldehyde resin (PTR)	149
Figure 4.44. FTIR spectra of pine type tannin-formaldehyde resin (PTR) and Zinc adsorbed pine type tannin-formaldehyde resin (PTR_Zn)	151
Figure 4.45. Absorption spectra for compound D	154

ACKNOWLEDGEMENTS

With deep sense of gratitude, I thank my supervisor Dr. Laleen Karunanayake, Senior Lecturer, Department of Chemistry, University of Sri Jayewardenepura for the keen interest, proper guidance, encouragement towards fulfilling my research work.

I would like to express gratitude to my co supervisor Dr. W S J Silva, Senior Lecturer, Department of Chemistry, University of Sri Jayewardenepura for his invaluable contribution to the Computational Chemistry part of this research.

I must also thank to the Vice Chancellor, Eastern University to grant me study leave to do this program.

I am thankful to Prof. S I Samarasinghe, Head of the Department of Chemistry, Prof. S P Deraniyagala, former Head of the Department of Chemistry and staff members of the department, whose integrated effort made the department a congenial place to perform research.

I wish to thank the National Science Foundation (Sri Lanka) for its financial support under Grant No. RG/2006/EB/04.

Finally, I am very grateful to my loving mother, wife Yalini, my son Shahaasan, daughter Sabthiha and all other well wishers for their prayers, inspiration, mental support and sacrifice that helped me to accomplish this research.

ABSTRACT

The main objective of this study was to find the feasibility of using locally available plant based tannin materials to use in place of phenol in the phenol-formaldehyde resins. This study deals with development of suitable sulfonated cross linked tannin-formaldehyde resin and tannin-phenol-formaldehyde resins as stable and reusable cation exchangers for the application in numerous industrial processes, e.g., water softening, separation of amino acids and epoxidation of oil.

In this study, fruit of Aralu tree, bark of the Kumbuk tree and fruits of Bulu tree were selected as tannin sources. The method of extraction of tannin was studied to obtain the highest possible yield. The extracted tannin was used to prepare tannin-phenol-formaldehyde resins with varying phenol to tannin ratios and their chemically modified forms.

The extracted tannins, tannin-phenol-formaldehyde (TPF) resins and their modified forms were characterized using UV-VIS, FTIR, ¹³C-NMR, rheological, SEM and DSC thermal analysis techniques. Polymerization mechanisms were studied using the above techniques supported by semi-empirical computational studies. In addition, the main electronic transitions for a flavan-3-ols type of compound involved in the UV-Visible absorption spectrum have been characterized.

The best procedure to extract tannin from three plant sources found to be using 80 % (v/v) methanol-water at pH value of 8 and 80 °C. Tannin extracted contained D-Catechin and Gallic acid related compounds. Total tannin contents of Aralu fruit, Kumbuk bark and Bulu fruit found to be 23.9, 17.9 and 17.1 %(w/w), respectively.

While NMR, FTIR spectroscopic methods confirmed the formation of phenolation of tannin and tannin-formaldehyde bond, the semi-empirical computational techniques

confirmed the formation of the tannin-formaldehyde bond via CH_2OCH_2 link initially at low temperatures, which, then, would convert to a CH_2 link after curing at $105\text{ }^\circ\text{C}$. In addition, the computational study shows that the reactivity of the catecholic B-ring of the tannin molecule could be increased by the incorporation of bivalent Zn^{2+} into the reaction system. The gel point of the reaction between tannin and formaldehyde reaction is found to be 4505 s from rheological analysis.

The resins were converted to their sulfonated forms to increase their ion exchange capacity as the exchange capacity found to be relatively low. Ion exchange capacities were tested for bivalent cations such as Zn^{2+} , Pb^{2+} , Ca^{2+} , Mg^{2+} and Cu^{2+} . In addition, as monovalent cations Na^+ , K^+ , NH_4^+ , and $(\text{CH}_3)_4\text{N}^+$ ions were also used for the study of exchange.

The maximum adsorption capacity was shown by the resin produced with tannin to phenol ratio of 1:0.5. This was explained by the formation of highly entangled molecules beyond this point using the T_g values obtained from DSC analysis. The highest adsorption capacities were revealed for Pb^{2+} adsorption in both sulfonated (0.610 meq/g) and unsulfonated (0.210 meq/g) resins. Further, more, it was found that the sulfonated tannin-phenol-formaldehyde resin follows Freundlich adsorption isotherm. The SEM analysis shows that lead ions adsorbed on the resin form multilayer structure showing a physical adsorption. In addition, the resin could be used in separation of amino acids.

It was found that the sulfonated resin produced could be used as a catalyst in various applications such as epoxidation of oils using per-acids and removal of water hardness. Further, the sulfonated resin was converted to an anion exchange resin. This modified resin could enhance its anion exchange capabilities.